Angewandte Chemie International Edition

Supported Catalysts

DOI: 10.1002/anie.201300130

Rationalization of Interactions in Precious Metal/Ceria Catalysts Using the d-Band Center Model

N. Acerbi, S. C. Edman Tsang,* G. Jones, S. Golunski, and P. Collier*

Catalysts consisting of precious metals (PMs) and ceria are widely used in heterogeneous catalysis, for example in applications such as three-way catalytic converters,[1] solid oxide fuel cells,[1] water–gas shift,[2] and CO oxidation.[3] In the past, the special synergy between PMs and ceria has most often been explained in terms of either "strong metal–support interaction" (SMSI)[4] or H_2 spillover.[5] However, Campbell has recently coined the term "electronic metal–support interaction" (EMSI),[6] a more specific description of the underlying cause for the often outstanding catalytic activity, which results from a high degree of contact between highly dispersed PM nanoparticles and ceria with a high surface area.

The SMSI effect was first reported in a seminar paper by Tauster et al.,[7] who found a loss of the ability for H_2 chemisorption for PM/TiO_2 catalysts (Pt, Pd, Rh, Ru, Ir or Os), when these were treated at high temperatures. This effect could be reversed by heating in O_2, which restored the H_2-chemisorption behavior of the catalyst.[7] One of the first hypotheses for explaining this effect was that the charge state of the metal was altered by the interaction with the electrons from the support underneath, thus leading to a modification of the ability for H_2 chemisorption, which also brought about a change in the catalytic properties of the metal.[8] However, later models established the concept of fractional coverage of the noble metal by partially reduced TiO_x species, leading to the blocking of sites for H_2 chemisorption.

In contrast to PM/TiO_2, the SMSI effect for PM/CeO_2 generally results in enhanced catalytic activity, even though the exposed PM surface area may be substantially reduced.[3] For a broad range of catalytic materials in which the PM is in contact with a redox-active oxide (including ceria), a reliable diagnostic of SMSI is to lower the temperature of the oxide reduction.[9] Although the precise role of the PM in facilitating the reduction of the redox-active metal oxide is still debated, two apparently alternative explanations for this phenomenon are most frequently proposed: 1) hydrogen spillover from the noble metal to the surface of the metal oxide,[10] and 2) an electronic interaction between the metal and the metal oxide.[3,11] The spillover model provides a physical mechanism by which the dissociation of molecular hydrogen on the surface of the noble metal generates highly mobile atomic hydrogen, which reduces the ceria by abstracting O^{2-} from its surface.[12] In the electronic-promotion model, the noble metal perturbs the electronic-band structure of the metal oxide, which is reduced directly by gas-phase H_2, without necessarily undergoing the exchange of surface chemical species between the noble metal and the redox-active oxide. Notably, we have reported that the reduction temperature of ceria close to precious-metal particles is dependent on the work function of the metal.[13] This observation provides compelling evidence that electronic interactions at the interface play a dominant role in the promotional effect of PMs dispersed on redox-active metal oxides.

In the 1950s, semiconductor theories of catalysis received much attention. These were based on concepts from solid-state physics,[14] and subsequently led to the development of the generally accepted "chemisorption" model. The nature of the molecule adsorbed at the surface of a semiconducting solid (often a redox-active metal oxide) depends on its redox potential relative to the upper edge of the valence band and bottom of the conductivity band in the solid. The position of these band states may be varied by the introduction of appropriate defects in the oxide through the incorporation of modifiers or promoters.[15] For instance by creating defects through reduction, the band states of reducible metal oxides can be changed, with an associated change in the interaction with the adsorbate, which might explain why the classic SMSI effect correlates with the reducibility of the oxide.[7,16] However, there are still unanswered questions about the SMSI effect, such as why it shows a strong correlation with redox-active oxide reducibility and how to explain the alteration in catalytic behavior.

In our previous work on electronic interactions between PMs and ceria,[13] we employed a model based on the "junction effect theory" proposed by Frost[17] to explain the metal/metal oxide interaction and the mechanism by which the noble metal electronically promotes a redox-active n-type metal oxide. This theory used the work function of the metal as electronic descriptor, as we have done in our previous work.[13,17]

---

[*] Dr. N. Acerbi, Dr. G. Jones, Dr. P. Collier
Johnson Matthey Technology Centre
Blount's Court Road, Sonning Common
Reading, RG4 9NH (UK)
E-mail: acerbn@matthey.com

Dr. N. Acerbi, Prof. S. C. E. Tsang
Wolfson Catalysis Centre, Inorganic Chemistry
Laboratory, University of Oxford
South Parks Road, Oxford, OX1 3QR (UK)
E-mail: edman.tsang@chem.ox.ac.uk

Dr. G. Jones
Department of Chemistry, University College of London
20 Gordon Street, London, WC1H 0AJ (UK)

Prof. S. Golunski
Cardiff Catalysis Institute, Cardiff University
Main Building, Park Place, Cardiff, CF10 3AT (UK)

Supporting information for this article is available on the WWW under http://dx.doi.org/10.1002/anie.201300130.

In the 1980s, Nørskov et al. introduced a supplementary band model based on DFT calculations, which describes how the changes in d-band centers of metal surfaces, surface alloys, and overlayers affect molecular adsorption in a semi-quantitative manner. The d-band center is considered an important parameter in determining the ability of the surface to bond to a number of adsorbates.[18] The model identified three properties contributing to the ability of the surface to make and break adsorbate bonds: 1) the position of the center (E_d) of the d-bands, 2) the degree of filling (f_d) of the d-bands, and 3) the coupling matrix element (V_{ad}) between the adsorbate states and the metal d-states. According to the model, as the d-band center shifts up (for example during alloying), a distinctive antibonding state appears above the Fermi level. The antibonding states above the Fermi level are empty, and the bond strength increases as their numbers increase. Therefore, strong bonding occurs if the antibonding states are shifted up relative to the Fermi level (and become empty), and weak bonding occurs if antibonding states are shifted down relative to the Fermi level (and become filled).[19] We believe that the electronic properties of both the precious metal and the redox-active metal oxide play a role in the improved reducibility of the latter, and ultimately in the occurrence of the generic SMSI effect. By using an electronic descriptor that correlates chemisorption energies to the electronic properties of the metal (i.e., d-band center), we are able to show that the reducibility of the redox-active metal oxide is strongly influenced by the electronic structure of the metal, and this in turn adds weight to the EMSI concept for explaining the enhanced catalytic activity associated with the precious metal/metal oxide interface.

The reduction characteristics of two consistent sets of $CeO_2/PM/SiO_2$ and $CeO_2/PM/Al_2O_3$ samples were investigated using temperature-programmed reduction (TPR), with particular focus on the effect of the PM on the reduction behavior of ceria. PM/SiO_2, PM/Al_2O_3, CeO_2/SiO_2, CeO_2/Al_2O_3, and CeO_2 were used for comparison to aid peak identification. The data validity, errors, and potential pitfalls of the TPR technique can be found in the Supporting Information. As examples, TPR profiles of $CeO_2/Pt/Al_2O_3$, $CeO_2/Ag/Al_2O_3$, and $CeO_2/Au/Al_2O_3$ are presented in Figure 1 and Table 1.

Table 1: Values of d-band centers calculated with d-band model[19] and measured temperatures of promoted reduction of ceria.

Metal	Center of d-band [eV]	*T* of reduction of PM [°C]		*T* of promoted reduction of surface ceria [°C]	
		Al_2O_3 supp.	SiO_2 supp.	Al_2O_3 supp.	SiO_2 supp.
Pt	−2.25	0	–[b]	110	80
Pd	−1.83	50	–[b]	140	100
Rh	−1.73	140	–[b]	200	125
Ru	−1.41	195	–[b]	220	155
Ag	−4.3	100	–[b]	200	173
Au[a]	−3.56	–	–[b]	140	–

[a] The synthesis of Au/SiO_2 and $CeO_2/Au/SiO_2$ was not successful because of a weak interaction between Au and the SiO_2 support, which led to a very poor dispersion of Au.

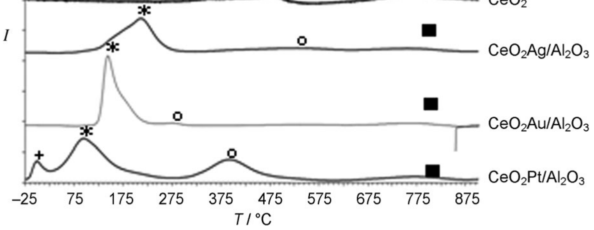

Figure 1. TPR profile of $CeO_2/PM/Al_2O_3$ (PM: Pt, Au, and Ag; +: PM oxide reduction). For ∗, ○, and ■, see the main text.

The TPR profiles of both $CeO_2/PM/SiO_2$ and $CeO_2/PM/Al_2O_3$ materials show ceria reduction peaks at lower temperature, a result of the combined reduction of PM and surface ceria, which is attributable to the abstraction of O^{2-} by hydrogen from surface ceria facilitated by the presence of the PM (∗).[20] Another peak is observed at intermediate temperature, resulting from the reduction of surface ceria that is more remote from the PM, that is, the peak originates from O^{2-} abstraction from surface ceria that is not in direct contact with PM nanoparticles (○).[20] Finally, a high-temperature peak is also observed because of the reduction of bulk ceria to Ce_2O_3 (■).[20] There are two exceptions: $CeO_2/Pt/SiO_2$, in which the reduction of bulk ceria is not observed, and $CeO_2/Ag/SiO_2$, which shows only a peak at low temperature related to the promoted reduction of surface ceria. (The interpretation of the TPR profiles for PM/Al_2O_3, PM/SiO_2, $CeO_2/PM/Al_2O_3$, and $CeO_2/Ag/SiO_2$ has been described in detail elsewhere[21]). $CeO_2/Au/Al_2O_3$ showed a convoluted reduction peak offsetting at 130 °C up to 250 °C with a maximum at 140 °C and a shoulder at 240 °C. The peak can be assigned to the promoted reduction of ceria, since the Au was found to be in a metallic form by TPR analysis of the ceria-free Au/Al_2O_3 sample (unpublished results). However, it has to be acknowledged that there may be some degree of uncertainty to the nature of this peak. Firstly, as it is highly convoluted, it could be composed of multiple peaks, and secondly it could be due to either an H_2 uptake/dissociation or to ceria reduction. In this work, our hypothesis is that the peak is due to ceria reduction.

The most apparent difference between the TPR profile for $CeO_2/Pt/Al_2O_3$ and those for $CeO_2/Ag/Al_2O_3$ and $CeO_2/Au/Al_2O_3$ is the fact that in the latter cases the majority of the ceria is reduced in a single step at moderate temperature.

In our previous work, we demonstrated that the change in ceria reducibility (as measured by TPR) as a result of the presence of PMs depends on the work function of the polycrystalline metal.[13] This correlation manifested itself as a linear dependence of ceria reducibility on the tabulated PM work function.[22] In the present work, the understanding of PM promotion of ceria reducibility was extended by establishing that the d-band center model[18,19] can also describe precious metal/ceria promotion. Figure 2 shows the temperature of the promoted ceria reduction for $CeO_2/PM/SiO_2$ and $CeO_2/PM/Al_2O_3$ plotted against the d-band center value

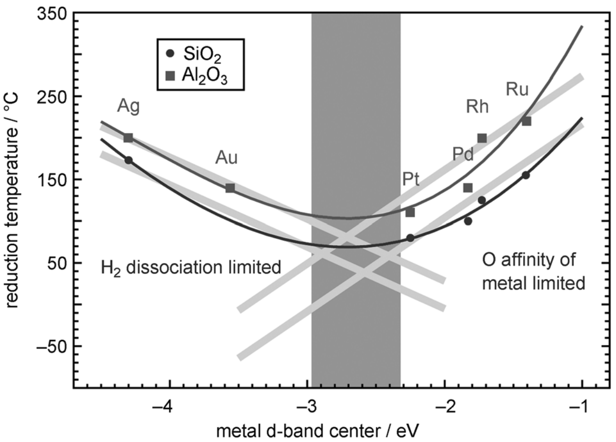

Figure 2. Correlation between the temperature of the promoted reduction of surface ceria and the calculated center of the noble metal d-band in CeO_2/PM/Al_2O_3.

taken from the report of Nørskov and co-workers.[19] An inverse "volcano"-type correlation is found for both CeO_2/PM/SiO_2 and CeO_2/PM/Al_2O_3, with the minimum centered slightly to the left of platinum, rising to Ag on the left and through Pd and Rh to Ru on the right.

The interpretation of the inverse volcano correlation found here can be based on chemisorption using the original interpretation of Nørskov and co-workers. The d-band center is defined by the Nørskov group[19] as the centroid of the d-type density states in an atomic sphere centered at a surface atom. This quantity is often referred to as C_d in the LMTO (linear muffin-tin orbitals) models. As this critically affects strength of chemisorption on a given surface, the inverse volcano relationship shown in Figure 2 can be explained in terms of the variable strengths of H_2 chemisorption on these surfaces (i.e., this is a spillover-type interpretation). Coinage metals, such as Ag and Au, weakly adsorb H_2, while early noble metals, such as Ru and Rh, strongly adsorb H_2. As a result, Pt appears to be optimal and forms surface bonds with hydrogen, enabling both the activation of the H_2 molecule as well as H-atom spillover.

In an attempt to further understand the "inverse" volcano plot obtained, the turnover frequency (k) in the form of the number of collisions that result in a reaction per second was calculated by using the Arrhenius equation in the following form:

$$k = \frac{k_b T}{h} e^{-E_a/RT} \tag{1}$$

where k_b is the Boltzmann constant expressed in $eV K^{-1}$; h is the Planck constant (eVs); E_a is the activation energy required to dissociate a molecule of H_2 on a metal surface; T is the temperature at which the ceria reduction occurs. The turnover frequency is dependent on both the temperature and the H_2 activation energy for Au and Ag metals (Table 2), where the dissociation of H_2 is not spontaneous on their surfaces, and a barrier needs to be overcome. Conversely, in the case of Pt, Pd, Rh, and Ru, once the metal oxide has been reduced to metal, the H_2 dissociates readily and no real energy barrier exists. Very interestingly, in the case of the Au-containing sample, the temperature at which the number of H_2 collisions results in a measurable dissociation rate, is the same as that of the ceria reduction peak in the CeO_2/Au/Al_2O_3 TPR profile. This phenomenon is observed in the case of Ag too, if an average of the reported activation energies calculated by modeling is taken into account. This observation strongly suggests that H_2 adsorption and dissociation are related to the facilitated reduction of ceria.

Table 2: Turnover of H_2 dissociation on Au and Ag metal surfaces. k = rate of collisions that result in reaction.

T [K]	Metal	E_a of H_2 dissociation	k [s^{-1}]
380	Au	1 eV[23]	0.432
400			2.09
420			8.75
420	Ag	1.11 eV[24]	0.552
440			2.30
460			8.50
480	Ag	≈125 kJ (1.29 eV)[25]	0.285
500			1.03
520			3.40

The analysis of the d-band center suggests that there are two limiting cases (given by the two slopes forming the volcano plot). In the weakly adsorbing system (Ag, Au), dihydrogen is hard to activate, while in the strongly adsorbing system, the dissociation of dihydrogen is no longer an activated process. Therefore, the hydrogen atom is able to adsorb on the surface as soon as it becomes available; the reduction in the Ag and Au systems is expected to be highly facilitated if the barrier for dihydrogen activation is overcome. This can be also distinguished by the single-step reduction in the TPR profiles (Figure 1). Thus, as suggested in Figure 2, the two limiting cases are represented by the two arms of the parabola. In the case of Ag and Au, the promoted reduction of surface ceria is limited by H_2 dissociation on metal particles. Conversely, for metals that spontaneously activate H_2 (Pt, Pd, Rh, and Ru), the ceria reduction is limited by the affinity of these metals for oxygen.

This hypothesis that adsorption and dissociation of H_2 on metal surfaces affects the promoted reduction of surface ceria is reinforced by the direct correlation between the reduction of PM oxide to metal and the promoted reduction of surface ceria. There is a clear linear relationship between the temperature of the reduction of the PM oxide (T_1) and the temperature of the promoted reduction of surface ceria (T_2) in the systems with Pt, Pd, Rh, and Ru (see Figure 3 and Table 3). T_1 and T_2 are increasing for Pt, Pd, Rh, and Ru, the order of which follows the inverse order the inverse order of their d-band center (see Table 1). Furthermore, the temperature of the reduction of PM oxide is always lower than the temperature of the promoted reduction of surface ceria. This correlation clearly shows that the reduction of the PM oxide is required to achieve the promoted reduction of surface ceria. Table 3 clearly shows that Ag does not follow the same trend

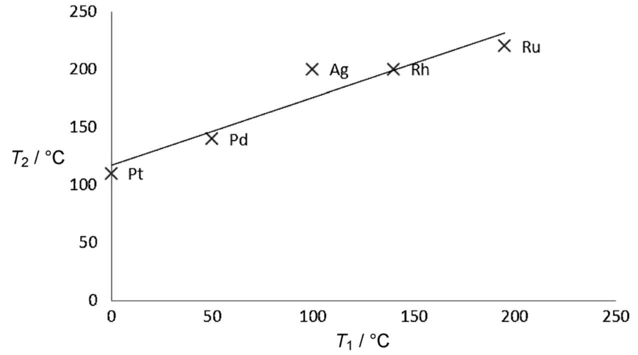

Figure 3. Correlation between the temperature of the PM oxide reduction (T_1) and the temperature of the promoted reduction of surface ceria (T_2) in $CeO_2/PM/Al_2O_3$.

Table 3: Comparison of reduction temperatures of the PM oxide and the ceria in contact with the PM.

Metal	*T* of metal reduction in PM/Al_2O_3 [°C]	*T* of promoted reduction of ceria in $CeO_2/PM/Al_2O_3$ [°C]	Temperature difference [°]
Pt	0	110	110
Pd	50	140	90
Rh	140	200	60
Ru	195	220	25
Ag	100	200	100

as the other precious metals (it is expected that Au does not follow this trend either), as the activation of dihydrogen is a limiting factor. It is therefore possible to predict that, if dissociative activation of H_2 was ruled out, as for example when a nondissociative reducing agent is used, that Ag and Au would be on the same trendline as Pt, Pd, Rh, and Ru, allowing the promoted reduction of ceria at even lower temperatures. This may well explain why Au/ceria catalysts are superior in reactions such as CO oxidation and water-gas shift.[26]

Finally, we suggest that the d-band center is a more effective electronic descriptor of the metal than the work function, which we used previously,[13] since it takes into account how the H_2 chemisorption is influenced by the structure of the metal. The chemisorptive aspect is not included by the definition of the work function. It appears that two cases can be distinguished, one in which the H_2 dissociation on the metal surface needs to be activated (Au and Ag), and the other in which such a process is spontaneous (Pt, Pd, Rh, and Ru).

We postulate that in heterogeneous catalysts such as those reported herein, in which the metal particles are partially exposed, the electronic properties of the metal drive H_2 chemisorption and dissociation on the metal surface. These steps ultimately correlate with the reducibility of the metal oxide, so that the spillover effect is a direct consequence of the electronic structure of the metal. However, model nanoparticle catalysts that consist of metal-core/ceria-shell, which completely exclude the metal surface from exposure to the gas phase, which could endorse the electronic interaction at the metal–ceria interface as the dominant effect.[27] For practical catalysts, a degree of metal exposure to hydrogen is unavoidable using the coating technique described herein. It is entirely possible that metal incorporation promotes both hydrogen spillover and an electronic modification, with the latter providing the driving force and the cause of the hydrogen spillover. SMSI is therefore ultimately related to the electronic nature of the catalytic system, while the spillover effect is only a consequence of it when the metal is partially exposed.

In addition to the correlation between the temperature of ceria reduction and the work function of the metal,[13] we have reported herein an inverse "volcano" correlation between the d-band center of the precious metal and the enhancement in ceria reducibility. The use of the d-band center as electronic descriptor of the electronic state of the metal was found to be more exhaustive than the correlation with the work function. It has allowed us to discriminate between two limiting cases in the series of metals we investigated:

1) Promoted reduction of surface ceria is limited by H_2 dissociation on Au and Ag particles.
2) In the cases of Pt, Pd, Rh, and Ru, where H_2 is readily dissociated on the metal, the limitation is the affinity of these metals for oxygen.

Additionally, the activated H_2 dissociation on Au and Ag results in "explosion" reduction during TPR, with the profile showing that most of the ceria present in the sample is reduced in one step. It is important to acknowledge that, in order to have an SMSI effect, a reduced metal surface in contact with a redox-active oxide (such ceria in this case) is needed. In conclusion, easily depicted models, such as hydrogen spillover, are clearly incomplete representations, and should probably no longer be used as stand-alone explanations for the enhanced reducibility and activity of precious metal/metal oxide catalysts.

Received: January 7, 2013
Revised: April 12, 2013
Published online: June 18, 2013

Keywords: ceria · d-band center · electronic effect · redox chemistry · supported catalysts

---

[1] A. Trovarelli, *Catalysis by Ceria and Related Materials*, Imperial College Press, London, **2002**.
[2] T. Bunluesin, R. J. Gorte, G. W. Graham, *Appl. Catal. B* **1998**, *15*, 107–114.
[3] S. E. Golunski, H. A. Hatcher, R. R. Rajaram, T. J. Truex, *Appl. Catal. B* **1995**, *5*, 367–376.
[4] S. Bernal, J. J. Calvino, M. A. Cauqui, J. M. Gatica, C. Larese, J. A. Perez Omil, J. M. Pintado, *Catal. Today* **1999**, *50*, 175–206.
[5] A. Bensalem, J. C. Muller, F. Bozon-Verduraz, *J. Chem. Soc. Faraday Trans.* **1992**, *88*, 153–154.
[6] C. T. Campbell, *Nat. Chem.* **2012**, *4*, 597–598.
[7] S. J. Tauster, S. C. Fung, R. L. Garten, *J. Am. Chem. Soc.* **1978**, *100*, 170–175.
[8] V. E. Herinch, P. A. Cox, *The Surface Science of Metal*, Cambridge University Press, Cambridge, **1996**.

[9] a) T. Beutel, H. Knözinger, A. V. Siborov, V. I. Zaikovskii, *J. Chem. Soc. Faraday Trans.* **1992**, *88*, 2775 – 2782; b) B. Harrison, A. F. Diwell, C. Hallett, *Platinum Met. Rev.* **1988**, *32*, 73 – 83.

[10] L. S. F. Feio, C. E. Hori, S. Damyanova, F. B. Noronha, W. H. Cassinelli, C. M. P. Marques, J. M. C. Bueno, *Appl. Catal. A* **2007**, *316*, 107 – 116.

[11] L. F. Liotta, A. Longo, A. Macaluso, A. Martorana, G. Pantaleo, A. M. Venezia, G. Deganello, *Appl. Catal. B* **2004**, *48*, 133 – 149.

[12] J. A. Wang, T. López, X. Bokhimi, O. Novaro, *J. Mol. Catal. A* **2005**, *239*, 249.

[13] N. Acerbi, S. C. Tsang, S. Golunski, P. Collier, *Chem. Commun.* **2008**, 1578 – 1580.

[14] a) K. Hauffe, *Adv. Catal.* **1955**, *7*, 213 – 257; b) F. F. Wolkenstein, *Adv. Catal.* **1957**, *9*, 807 – 817.

[15] J. Haber, *Catal. Today* **2009**, *142*, 100 – 113.

[16] L. Haller, *J. Catal.* **2003**, *216*, 12 – 22.

[17] J. Frost, *Nature* **1988**, *334*, 577 – 580.

[18] S. Holloway, B. I. Lundqvist, J. K. Nørskov, in *Proceedings of the 8th International Congress on Catalysis*, *Vol. 4*, Verlag Chemie, Weinheim, Berlin, **1984**, pp. 85 – 95.

[19] A. Ruban, B. Hammer, P. Stoltze, H. L. Skriver, J. K. Nørskov, *J. Mol. Catal. A* **1997**, *115*, 421 – 429.

[20] a) S. Damyanova, J. M. C. Bueno, *Appl. Catal. A* **2003**, *253*, 135 – 150; b) E. Rocchini, M. Vicario, J. Llorca, C. de Leitenburg, G. Dolcetti, A. Trovarelli, *J. Catal.* **2002**, *211*, 407 – 421; c) J. Silvestre-Albero, F. Rodrígue-Reinoso, A. Sepúlveda-Escribano, *J. Catal.* **2002**, *210*, 127 – 136; d) M. J. Tiernan, O. E. Finlayson, *Appl. Catal. B* **1998**, *19*, 23 – 35.

[21] N. Acerbi, S. Golunski, S. C. Tsang, H. Daly, C. Hardacre, R. Smith, P. Collier, *J. Phys. Chem. C* **2012**, *116*, 13569 – 13583.

[22] H. E. Michaelson, *J. Appl. Phys.* **1977**, *48*, 4729 – 4734.

[23] B. Hammer, J. K. Nørskov, *Nature* **1995**, *376*, 238 – 240.

[24] Y. Xu, J. Greeley, M. Mavrikakis, *J. Am. Chem. Soc.* **2005**, *127*, 12823 – 12827.

[25] A. B. Mohammad, K. Hwa Lim, I. V. Yudanov, K. M. Neyman, N. Rösch, *Phys. Chem. Chem. Phys.* **2007**, *9*, 1247 – 1254.

[26] a) W. Deng, J. De Jesus, H. Saltsburg, Flytzani-Stephanopoulos, *Appl. Catal. A* **2005**, *291*, 126 – 135; b) M. Haruta, T. Kabayashi, H. Sano, N. Yameda, *Chem. Lett.* **1987**, 405.

[27] C. M. Y. Yeung, K. M. K. Yu, Q. J. Fu, D. Thompsett, M. I. Petch, S. C. Tsang, *J. Am. Chem. Soc.* **2005**, *127*, 18010 – 18011.